

Suppression and revival of long-range ferromagnetic order in the multiorbital Fermi–Hubbard model

Andrii Sotnikov,^{1,2,*} Agnieszka Cichy,^{3,4} and Jan Kuneš¹

¹*Institute of Solid State Physics, TU Wien, Wiedner Hauptstr. 8, 1020 Vienna, Austria*

²*Akhiezer Institute for Theoretical Physics, NSC KIPT, Akademichna Str. 1, 61108 Kharkiv, Ukraine*

³*Faculty of Physics, Adam Mickiewicz University, Umultowska 85, 61-614 Poznan, Poland*

⁴*Institut für Physik, Johannes Gutenberg-Universität Mainz, Staudingerweg 7, D-55099 Mainz, Germany*

(Dated: November 7, 2018)

By means of dynamical mean-field theory allowing for complete account of SU(2) rotational symmetry of interactions between spin-1/2 particles, we observe a strong effect of suppression of ferromagnetic order in the multiorbital Fermi-Hubbard model in comparison with a widely-used restriction to density-density interactions. In case of orbital degeneracy, we show that the suppression effect is the strongest in the two-orbital model (with effective spin $S_{\text{eff}} = 1$) and significantly decreases when considering three orbitals ($S_{\text{eff}} = 3/2$), thus magnetic ordering can effectively revive for the same range of parameters, in agreement with arguments based on vanishing of quantum fluctuations in the limit of classical spins ($S_{\text{eff}} \rightarrow \infty$). We analyze a connection to the double-exchange model and observe high importance of spin-flip processes there as well.

I. INTRODUCTION

Symmetry, its discrete or continuous nature, and its explicit or spontaneous breaking play a crucial role in physics. In condensed matter theory, Heisenberg and Ising models are distinctive examples of systems possessing continuous and discrete spin symmetry, respectively. While the spontaneous breaking of spin symmetry plays a central role in observations of phase transitions and emerging gapless collective modes, its explicit analog is less “charming” and usually originates from the internal or external source fields, sample imperfections, or simplifications required to proceed with the corresponding theoretical description.

Long-range ferromagnetic (FM) order is prominent realization of spontaneously broken symmetry responsible for many important physical phenomena, e.g., the colossal magnetoresistance effect in manganites [1]. In a search of a representative lattice system of itinerant interacting particles supporting the FM ground state, a single-band Hubbard model can be suggested as the simplest one. However, as emphasized and studied in detail in Ref. [2], this is *not a generic* model of ferromagnetism, since for realistic lattice geometries (without loop structures and additional nearest-neighbor “biasing” interactions) the corresponding FM ground state can only emerge in the Nagaoka’s limit ($U = \infty$). The next by simplicity, the two-orbital Hubbard model, provides a minimal number of necessary ingredients (in particular, a local nonzero Hund’s coupling) to support the suggested type of magnetic ordering.

Nowadays, dynamical mean-field theory (DMFT) [3] is a powerful nonperturbative theoretical approach to describe physics of strongly-correlated materials including transitions between different thermodynamic phases. In

a number of previous DMFT studies analyzing ferromagnetic instability in the two-band Hubbard models the computational procedure was restricted to the density-density interactions [4–8]. Although this simplification essentially reduces the computational cost in the corresponding impurity solvers, it can lead to imprecise treatment of systems, especially close to the critical regime (see, e.g., Ref. [9] for a recent material-oriented analysis). Therefore, a significant effort has been made to account for the full rotational symmetry of two-particle interactions [10–16] in the corresponding numerical procedures.

In parallel to the progress of DMFT and other theoretical approaches, ultracold atoms in optical lattices [17] have become a universal and very accurate experimental tool for gaining new insights in a rich family of the Hubbard-type models. In these systems, a degree of freedom associated with the electron spin can be attributed to atoms in different internal states (i.e., the *pseudospin* concept is widely applied). This results in a relatively large tunability — at will, the spin symmetry can be explicitly broken or restored with an ultimate accuracy by a proper experimental setting [18, 19]. In particular, recent experiments with ^{173}Yb and ^{87}Sr atoms [20–22] show the corresponding capability to realize two-orbital Hubbard models with the FM-type Hund’s coupling and SU(N)-symmetric interactions of pseudospin flavors.

The purpose of the present paper is to analyze in a systematic way the effect of interaction parametrization — with the SU(2) spin-rotational symmetry or lower — on FM ordering in the multiorbital Hubbard models. Starting with degenerate orbitals we introduce a crystal field in order to link the metallic Stoner-type FM phase of the Hubbard model with overlapping bands to the FM phase of the double-exchange (DE, or the Kondo-lattice) model. The latter has a long history [23] and it is widely applied to describe FM ordering and related effects in manganites. The model studies by means of DMFT have already uncovered important effects of electronic correlations [24, 25] and spin fluctuations [26] on FM ordering

* sotnikov@ifp.tuwien.ac.at

in the DE regime.

The paper is organized as follows. In Sec. II we introduce the theoretical model and specify relevant details of the applied numerical approach. We analyze the FM instability starting from the case of degenerate orbitals in Sec. III A and proceed further with introducing the chemical potential imbalance (i.e., a nonzero crystal field) in Sec. III B. The main results are summarized in Sec. IV.

II. MODEL AND METHOD

We consider the Fermi–Hubbard model with multiple ($m = 2, 3$) orbitals described by the Hamiltonian

$$\begin{aligned} \mathcal{H} = & \sum_{\mathbf{k}\sigma} \sum_{\gamma=1}^m (\epsilon_{\mathbf{k}\gamma} + \mu_{\gamma}) c_{\mathbf{k}\gamma\sigma}^{\dagger} c_{\mathbf{k}\gamma\sigma} + U \sum_{i\gamma} n_{i\gamma\uparrow} n_{i\gamma\downarrow} \\ & + U' \sum_{i\sigma,\gamma < \gamma'} n_{i\gamma\sigma} n_{i\gamma'\bar{\sigma}} + (U' - J) \sum_{i\sigma,\gamma < \gamma'} n_{i\gamma\sigma} n_{i\gamma'\sigma} \\ & + \alpha J \sum_{i,\gamma < \gamma'} (c_{i\gamma\uparrow}^{\dagger} c_{i\gamma'\downarrow}^{\dagger} c_{i\gamma\downarrow} c_{i\gamma'\uparrow} + \text{H.c.}) \\ & + \alpha' J \sum_{i,\gamma < \gamma'} (c_{i\gamma\uparrow}^{\dagger} c_{i\gamma'\downarrow}^{\dagger} c_{i\gamma\downarrow} c_{i\gamma'\uparrow} + \text{H.c.}). \end{aligned} \quad (1)$$

The first term includes free-particle energies $\epsilon_{\mathbf{k}\gamma}$, chemical potentials μ_{γ} and fermionic creation (annihilation) operators $c_{\mathbf{k}\gamma\sigma}^{\dagger}$ ($c_{\mathbf{k}\gamma\sigma}$) of electrons on the orbital γ with the spin $\sigma = \uparrow, \downarrow$ (and its opposite $\bar{\sigma} = \downarrow, \uparrow$) and quasi-momentum \mathbf{k} . U is the intraorbital interaction amplitude and J characterizes local (i is the lattice site index) ferromagnetic ($J > 0$) Hund’s coupling. Here and below, we use the parametrization $U' = U - 2J$, which is generally valid for all electron–electron interactions that are rotationally invariant in real space. The coefficients $\alpha, \alpha' \in [0, 1]$ can be set, in principle, independently of each other. At $\alpha = \alpha'$, the two limiting cases with $\alpha = 0$ and $\alpha = 1$ correspond to the so-called density–density (Ising-type) and Slater–Kanamori (SK) parametrization of interactions. We also restrict ourselves to all positive interaction amplitudes that results in limitations $U > 0$ and $J \leq U/3$.

The Hamiltonian (1) allows for a separate analysis of spin and orbital sectors. Since the symmetry of the latter is almost irrelevant for the current study, we omit its discussion [27] for simplicity. Therefore, it is sufficient to point out briefly the influence of the Ising-anisotropy parameter α on the symmetry of the spin sector. In particular, at $\alpha = 1$ the model becomes SU(2) symmetric with respect to rotations in spin space. Any other value of α ($0 \leq \alpha < 1$) lowers the symmetry of the spin part to the $\mathbb{Z}_2 \times \text{U}(1)$ group, where \mathbb{Z}_2 corresponds to reflections of the type $c_{\gamma\uparrow} \rightarrow c_{\gamma\downarrow}$ and U(1) suggests the invariance of the Hamiltonian under rotations around the z quantization axis, $(c_{\gamma\uparrow}, c_{\gamma\downarrow}) \rightarrow (e^{i\phi} c_{\gamma\uparrow}, e^{-i\phi} c_{\gamma\downarrow})$.

In the DMFT analysis of magnetic ordering in the system under study, we employ two types of solvers

for the auxiliary Anderson impurity problem. We use the continuous-time hybridization expansion quantum Monte Carlo (CT-HYB) impurity solver provided via the `w2dynamics` software package [28], which includes necessary generalizations introduced in Refs. [10, 11, 15]. The second option, the exact diagonalization (ED) solver is based on extensions discussed in Refs. [16, 29]. The maximal number of effective bath orbitals per each orbital and spin flavor in ED is limited in the present study to $n_s = 4$ (for $m = 2$) and $n_s = 3$ (for $m = 3$) [30]. Since the used CT-HYB solver does not suffer from a sign problem [10], we use its output for the resulting diagrams and graphical dependencies and the output from the ED solver as a supplementary source supporting main observations.

For simplicity and general analysis purpose, it is sufficient to restrict below to a semicircular density of states $D(\epsilon) = (1/2\pi t^2) \sqrt{4t^2 - \epsilon^2}$ and to set the hopping amplitude t as the scaling unit ($t \equiv t_m = 1$) in all energy-related quantities (e.g., the bandwidth for the non-interacting system thus becomes $W = 4$). Note that estimates for more realistic lattice geometries can usually be performed by a proper rescaling of quantities with respect to the coordination number z of the actual lattice ($t \rightarrow \sqrt{z}t$) [31]. For example, in simple cubic (sc) lattice geometry with $z = 6$, the energy-related parameter P (e.g., critical temperature or interaction strength) becomes $P_{\text{sc}} \approx \sqrt{6} P_{\text{Bethe}}$.

The FM instability is analyzed in two ways: by direct measurements of uniform magnetizations (both with the CT-HYB and ED impurity solvers) and by analyzing uniform susceptibilities in the symmetric phase with an external magnetic field (with the ED solver, see, e.g., Ref. [7]). Due to restricting to the single-site DMFT and to the hybridization functions that are diagonal in orbital and spin indices, we do not have a direct access in measurements of other potentially competing (e.g., canted antiferromagnetic, Ruderman–Kittel–Kasuya–Yosida coupling, spin-orbit pairing, and excitonic) instabilities.

III. RESULTS

A. Degenerate orbitals

We start our analysis from the moderate regime of parameters U and J that are commonly used in theoretical studies of strongly-correlated electron systems with a multiple number of orbitals. By fixing $U = 12$ and $J = U/4$ we obtain phase diagrams for the degenerate orbitals shown in Fig. 1. The most striking feature is that in case of two-orbital system FM order completely vanishes in the SU(2)-symmetric ($\alpha = 1$) limit. This is in contrast to previous expectations (based on DMFT analysis with the density–density interactions only, see Ref. [4]) that the spin-flip term has no strong effect on critical temperatures at intermediate coupling. In fact, it does and, as we see from comparison with the three-band model at

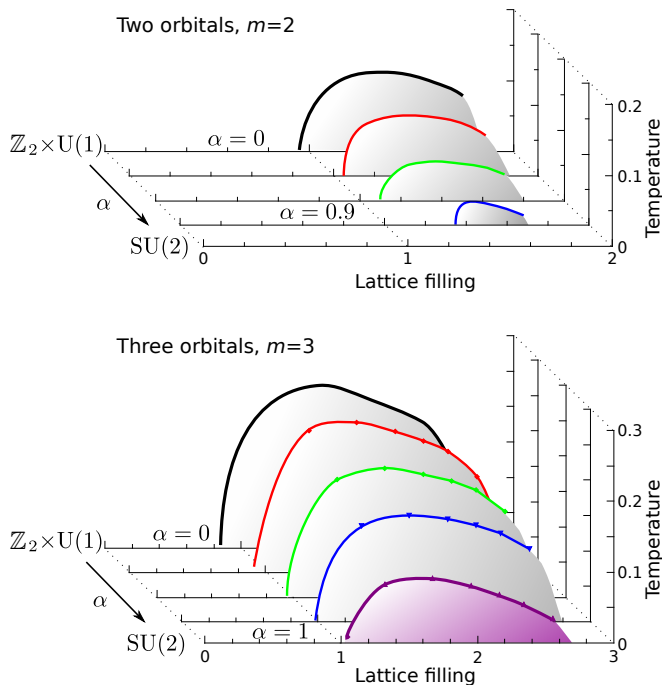


FIG. 1. Phase diagrams indicating evolution of FM phases under the change of the Ising anisotropy parameter α ($\alpha = 0, 0.6, 0.8, 0.9, 1$ from back to front) at $U = 12$ and $J = 3$.

same values of couplings, FM ordering is sensitive to the number of active orbitals included into description. We address this effect to suppression of quantum fluctuations with an increase of the number of orbitals, i.e., effective spins become more classical (see, e.g., Ref. [32]).

Next, we are interested to determine the critical values of the interaction amplitudes. We use two parameterizations, $\alpha = 0$ and $\alpha = 1$ (as the most relevant limits), and fix the temperature to $T = 0.025$, while allowing for different interaction amplitudes U and J . The corresponding results are summarized in Fig. 2. In the diagram for the two-orbital model, we observe a strong suppression of the FM phase by the spin-flip term. This effect is already significantly reduced in the three-orbital model. Note that, similarly to arguments for the single-band $SU(2)$ -symmetric Hubbard model [2], the results confirm absence of the FM instability at $U < \infty$ in higher-symmetric (single-band) $SU(2m)$ -symmetric models, corresponding to the $J \rightarrow 0$ limit in Fig. 2.

The parametrization of interactions significantly affects not only the positions of the FM phase boundaries, but also single-particle observables that are relevant in physics of so-called Hund's metals [33–35] in the PM regime. In particular, by varying the Ising-anisotropy parameter α from zero to one we observe sizable changes in the low-energy behavior of the self-energy that determines relevant observables, such as the effective mass and the lifetime of quasiparticles. Following Ref. [36], we use the polynomial fit for the first six poles of the imaginary part of the self-energy $\Sigma(i\omega_n)$ on the

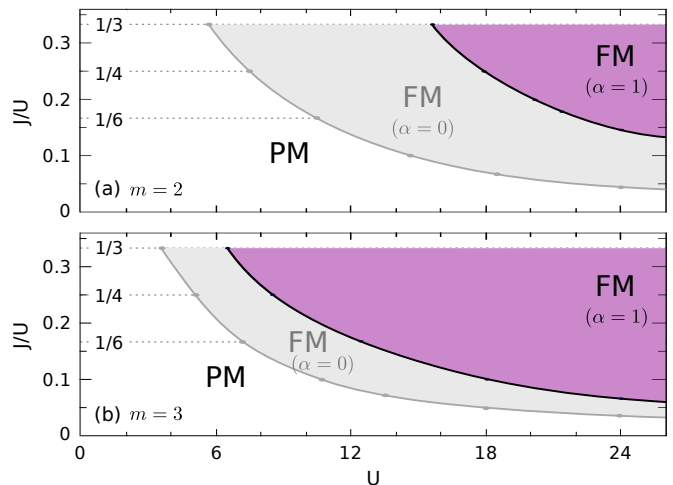


FIG. 2. U - J phase diagrams of the degenerate two-orbital (a) and three-orbital (b) models in the low-temperature region ($T = 0.025$) at the lattice filling $n = 1.5$.

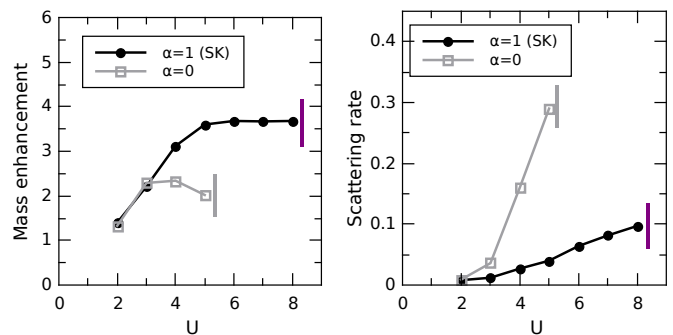


FIG. 3. Dependencies of the mass enhancement and the quasiparticle scattering rate (inverse lifetime) on the interaction strength U for the $m = 3$ model in the PM regime at $n = 2$, $J = U/4$, and $T = 0.025$. The vertical bars indicate the corresponding FM phase boundaries.

Matsubara axis, $\omega_n = \pi(2n + 1)T$ with $n = 0, 1, 2, \dots$. Then, basing on the fitting function, the mass enhancement (the inverse quasiparticle weight) is estimated as $Z^{-1} = 1 - d \text{Im}[\Sigma(i\omega_n)]/d\omega_n|_{\omega_n \rightarrow 0}$. The quasiparticle scattering rate Γ (the inverse lifetime) is obtained according to the relation $\Gamma Z^{-1} = - \text{Im}[\Sigma(i\omega_n)]|_{\omega_n \rightarrow 0}$. As it is shown in Fig. 3, the difference in the observables from two limits becomes maximally pronounced in the proximity of the FM($\alpha = 0$) phase boundaries. At $m = 3$, $n = 2$, and $\alpha = 1$ (in contrast to the $\alpha = 0$ parametrization), we also observe a good quantitative agreement in positions of transition lines from the FM to metallic PM phase to those that were obtained for the ruthenium perovskite CaRuO_3 [36].

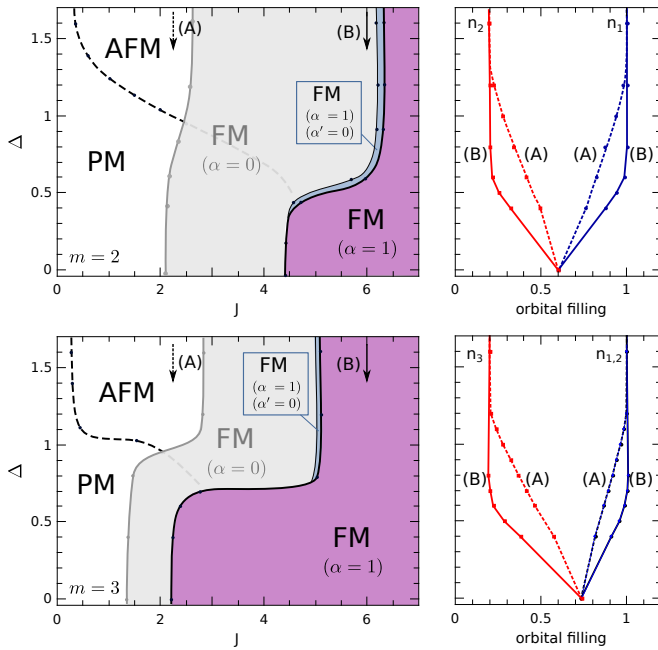


FIG. 4. Left: J - Δ phase diagrams of the two-orbital ($m = 2$) and three-orbital ($m = 3$) models at the lattice fillings $n = 1.2$ and $n = 2.2$, respectively. Right: the orbital occupations n_γ along the vertical lines indicated by arrows on the corresponding diagrams at $J = 2.25$ (A, dashed lines) and $J = 5.5$ (B, solid lines). The U/J ratio is kept fixed, $U = 4J$, and $T = 0.025$ everywhere.

B. Split orbitals

Now, we analyze the stability of FM phases against changes in orbital occupations. This is achieved by introducing a crystal field $\Delta = \mu_m - \mu_\gamma$ ($\gamma = 1, \dots, m-1$), which splits off one orbital from the rest. We fix the population $n = m - 1 + \delta$ so that in the limit of large U and $\Delta > t_\gamma$ (DE regime) the lower degenerate band becomes half-filled, while the population of the split-off band reaches $\delta = 0.2$. First, to have a connection with results of Sec. III A, we keep all bandwidths equal, $W_\gamma = W_m = 4$ and vary Δ . Second, we vary the bandwidth of the lower degenerate bands for the fixed Δ .

In Fig. 4 we show the FM phase boundaries as functions of Δ and J . Similarly to results shown in Sec. III A, the effect of restoring of the spin-rotational symmetry by $\alpha = 1$ is pronounced in the $m = 2$ model and decreases when $m = 3$. In contrast, even in the presence of the splitting $\Delta > 0$, the pair-hopping term (included by $\alpha' = 1$) has almost vanishing contributions to the changes of phase boundaries (see narrow regions between FM with $\alpha = 0$ and $\alpha = 1$ in Fig. 4) in the regimes under study.

The shapes of the FM phase boundaries in Fig. 4 defy the naive expectations that the crystal field should stabilize the FM order due to breaking of the orbital symmetry of the Hamiltonian (1). According to our analysis, the effect of relatively large suppression of the FM phase

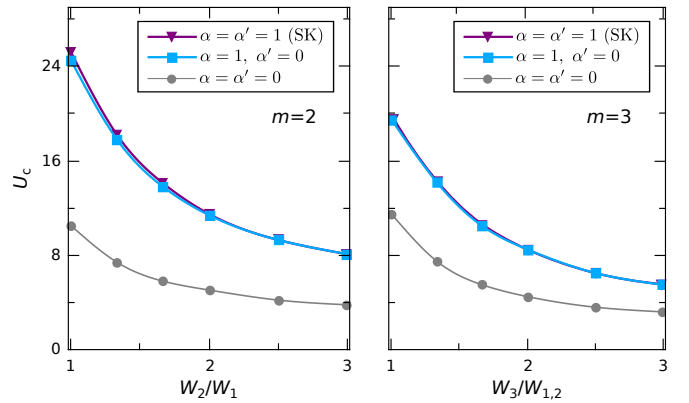


FIG. 5. Dependencies of the critical interaction strengths U_c for FM ordering on the bandwidth asymmetry in two-orbital (left) and three-orbital (right) Hubbard models at $\Delta = 1.2$ and other parameters as in Fig. 4. The hopping amplitude in the upper band is fixed to $t_m = 1$.

in the DE regime of Fig. 4 ($\Delta \gtrsim 1$) is caused by an additional competition with the antiferromagnetic (AFM) ordering that originates from the nearest-neighbor kinetic exchange (also called superexchange) within the lowest effective band that becomes half-filled.

To discuss the influence of AFM correlations, it is useful map the Hamiltonian (1) to an effective Kondo-lattice model with an additional AFM coupling term characterized by the amplitude \mathcal{J}_A (similar models were also the subject of theoretical studies [37–40]),

$$\mathcal{H}_{\text{eff}} = - \sum_{\gamma=1}^m t_\gamma \sum_{\langle ij \rangle \sigma} c_{i\gamma\sigma}^\dagger c_{j\gamma\sigma} - J_K \sum_i \mathbf{s}_i \cdot \mathbf{S}_i + \mathcal{J}_A \sum_{\langle ij \rangle} \mathbf{S}_i \cdot \mathbf{S}_j, \quad (2)$$

where the “localized” spins, $\mathbf{S}_i = \frac{1}{2} \sum_{\gamma=1}^{m-1} c_{i\gamma\sigma}^\dagger \boldsymbol{\tau}_{\sigma\sigma'} c_{i\gamma\sigma'}$, and “itinerant” spins, $\mathbf{s}_i = \frac{1}{2} c_{im\sigma}^\dagger \boldsymbol{\tau}_{\sigma\sigma'} c_{im\sigma'}$, are expressed in terms of Pauli matrices $\boldsymbol{\tau}$, $\langle ij \rangle$ indicates summation over nearest-neighbor lattice sites, and the so-called Kondo coupling J_K is related here to the Hund’s coupling J of Eq. (1) by renormalization $J_K = 4J/(m-1)$. In the strong-coupling limit for lower orbitals, the AFM coupling constant scales as $\mathcal{J}_A \propto t_\gamma^2/U$ ($\gamma < m$). Therefore, to suppress the influence of the last term in this regime, it is sufficient to decrease the corresponding bandwidths W_γ ($\gamma < m$), while keeping other parameters fixed.

The DMFT results in Fig. 5 exhibit an enhancement of the FM instability due to suppression of its main competitor, the AFM coupling, with the band asymmetry. As before, from direct comparison of $\alpha = 0$ and $\alpha = 1$ parameterizations we observe a more pronounced effect of SU(2) spin symmetry in the two-orbital model ($m = 2$) that decreases with inclusion of an additional orbital flavor into the lower effective band ($m = 3$).

To keep the study consistent, we do not extend our

current description to larger degeneracies of orbitals, but the observed behavior allows to make a useful extrapolation from the point of view of solid-state realizations. For systems characterized by the electronic d -orbitals in cubic perovskite crystal structures (and in manganites, in particular), the typical band asymmetry can be roughly estimated as $W_{e_g}/W_{t_{2g}} \approx 2$. Assuming triple degeneracy of the lower (t_{2g}) and double degeneracy of the higher (e_g) states and $n = 3 + \delta$, the corrections to characteristic critical values due to spin-flip processes are expected to be still noticeable but, presumably, will not exceed 30%. The analyzed dependencies also suggest that the antiferromagnetic correlations within the t_{2g} orbitals play an important role in physics of manganites and related compounds, thus must be properly accounted for.

IV. SUMMARY AND OUTLOOK

We studied the influence of spin symmetry (in particular, presence of the spin-flip term) in the interaction part of the Hamiltonian on the FM instability in the multi-orbital Hubbard model by means of DMFT. We observe strong effects of suppression of FM phases when accounting for full spin-rotational symmetry in the two-orbital systems (in contrast to weaker effects for AFM ordering [14, 16]). By considering the three-orbital model, it is shown that these effects become weaker (i.e., FM ordering effectively revives) with an increase of the number of active orbitals that agrees well with arguments based on suppression of quantum fluctuations due to approaching the limit of classical spins. The analysis was extended to the case of split orbitals, where the corresponding transition from the Stoner to the double-exchange regime of FM ordering is observed, but the suppression effect originating from inclusion of the spin-flip processes remains significant.

The applied approach was restricted to measurements of observables diagonal in spin and orbital indices. Therefore, a number of instabilities with more complex structure (e.g., possible canted AFM ordering in the DE

regime) were not studied directly. In view of recent developments in DMFT schemes with corresponding extensions [6, 41, 42], research directions aiming to obtain more detailed phase diagrams in the regimes under study look realistic.

The results for the two-band model are also important from the viewpoint of the ultracold-atom experiments focused on approaching the ferromagnetic Kondo-lattice regime in optical lattices. Preliminary estimates for different parameterizations of interactions, $U \ll J \lesssim U'$, i.e., different from the current study but closer to the experimentally accessible values [20, 22], show that the influence of spin-flip terms remains crucial for a determination of critical parameters for FM ordering. It is also interesting to study the influence of quantum fluctuations in two-orbital models with $SU(N)$ -symmetric interactions, where magnetic ordering is expected to be suppressed with an increase of N (number of pseudospin flavors), in contrast to the studied direction of $SU(2)$ -symmetric interactions and increasing m (number of active orbitals), where FM phases become stabilized with m .

ACKNOWLEDGMENTS

The authors thank A. Golubeva, A. Hariki, and P. van Dongen for fruitful discussions. We highly appreciate technical assistance by A. Hausoel, P. Gunacker, and G. Sangiovanni with the `w2dynamics` package. A.S. and J.K. acknowledge funding of this work from the European Research Council (ERC) under the European Union's Horizon 2020 research and innovation program (Grant Agreement No. 646807-EXMAG). A.C. acknowledges funding of this work by the National Science Centre (NCN, Poland) under grant: UMO-2017/24/C/ST3/00357. Access to computing and storage facilities provided by the Vienna Scientific Cluster (VSC) is greatly appreciated. The calculations were also performed at the Poznan Supercomputing and Networking Center (EAGLE cluster).

-
- [1] Y. Moritomo, A. Asamitsu, H. Kuwahara, and Y. Tokura, *Nature* **380**, 141 (1996).
 - [2] M. Kollar, R. Strack, and D. Vollhardt, *Phys. Rev. B* **53**, 9225 (1996).
 - [3] A. Georges, G. Kotliar, W. Krauth, and M. J. Rozenberg, *Rev. Mod. Phys.* **68**, 13 (1996).
 - [4] K. Held and D. Vollhardt, *Eur. Phys. J. B* **5**, 473 (1998).
 - [5] S. Hoshino and P. Werner, *Phys. Rev. Lett.* **115**, 247001 (2015).
 - [6] S. Hoshino and P. Werner, *Phys. Rev. B* **93**, 155161 (2016).
 - [7] A. Cichy and A. Sotnikov, *Phys. Rev. A* **93**, 053624 (2016).
 - [8] A. Sotnikov and J. Kuneš, *Phys. Rev. B* **96**, 245102 (2017).
 - [9] A. Hausoel, M. Karolak, E. Sasioglu, A. Lichtenstein, K. Held, A. Katanin, A. Toschi, and G. Sangiovanni, *Nat. Comm.* **8**, 16062 (2017).
 - [10] P. Werner and A. J. Millis, *Phys. Rev. B* **74**, 155107 (2006).
 - [11] A. M. Läuchli and P. Werner, *Phys. Rev. B* **80**, 235117 (2009).
 - [12] C.-K. Chan, P. Werner, and A. J. Millis, *Phys. Rev. B* **80**, 235114 (2009).
 - [13] R. Peters and T. Pruschke, *Phys. Rev. B* **81**, 035112 (2010).
 - [14] A. E. Antipov, I. S. Krivenko, V. I. Anisimov, A. I. Lichtenstein, and A. N. Rubtsov, *Phys. Rev. B* **86**, 155107 (2012).
 - [15] N. Parragh, A. Toschi, K. Held, and G. Sangiovanni,

- Phys. Rev. B **86**, 155158 (2012).
- [16] A. Golubeva, A. Sotnikov, A. Cichy, J. Kuneš, and W. Hofstetter, *Phys. Rev. B* **95**, 125108 (2017).
- [17] I. Bloch, J. Dalibard, and W. Zwerger, *Rev. Mod. Phys.* **80**, 885 (2008).
- [18] S. Taie, Y. Takasu, S. Sugawa, R. Yamazaki, T. Tsujimoto, R. Murakami, and Y. Takahashi, *Phys. Rev. Lett.* **105**, 190401 (2010).
- [19] J. S. Krauser, J. Heinze, N. Fläschner, S. Götze, O. Jürgensen, D.-S. Lühmann, C. Becker, and K. Sengstock, *Nat. Phys.* **8**, 813 (2012).
- [20] F. Scazza, C. Hofrichter, M. Höfer, P. C. De Groot, I. Bloch, and S. Fölling, *Nat. Phys.* **10**, 779 (2014).
- [21] X. Zhang, M. Bishof, S. L. Bromley, C. V. Kraus, M. S. Safronova, P. Zoller, A. M. Rey, and J. Ye, *Science* **345**, 1467 (2014).
- [22] L. Riegger, N. Darkwah Oppong, M. Höfer, D. R. Fernandes, I. Bloch, and S. Fölling, *ArXiv e-prints* (2017), [arXiv:1708.03810](https://arxiv.org/abs/1708.03810) [cond-mat.quant-gas].
- [23] C. Zener, *Phys. Rev.* **82**, 403 (1951).
- [24] K. Held and D. Vollhardt, *Phys. Rev. Lett.* **84**, 5168 (2000).
- [25] Y. Imai and N. Kawakami, *J. Phys. Soc. Jpn.* **69**, 3063 (2000).
- [26] K. Nagai, T. Momoi, and K. Kubo, *J. Phys. Soc. Jpn.* **69**, 1837 (2000).
- [27] See Refs. [6, 35] for details.
- [28] M. Wallerberger, A. Hausoel, P. Gunacker, A. Kowalski, N. Parragh, F. Goth, K. Held, and G. Sangiovanni, *ArXiv e-prints* (2018), [arXiv:1801.10209](https://arxiv.org/abs/1801.10209) [cond-mat.str-el].
- [29] A. Sotnikov, *Phys. Rev. A* **92**, 023633 (2015).
- [30] The limitations in ED are caused by the exponential growth of the corresponding Hilbert space with the total number of states $\mathcal{N} = 2mn_s$. We systematically verified that the used maximal numbers of n_s are sufficient for ED and CT-HYB results to fall into a good agreement of the order of the line width in figures corresponding to the regime of overlapping bands. At lower n_s values or in the DE regime, the deviations become more noticeable.
- [31] N. Blümer and E. V. Gorelik, *Phys. Rev. B* **87**, 085115 (2013).
- [32] P. Fazekas, *Lecture Notes on Electron Correlation and Magnetism* (World Scientific, Singapore, 1999) Chap. 6, pp. 263–340.
- [33] Z. P. Yin, K. Haule, and G. Kotliar, *Nat. Mat.* **10**, 932 (2011).
- [34] L. de' Medici, J. Mravlje, and A. Georges, *Phys. Rev. Lett.* **107**, 256401 (2011).
- [35] A. Georges, L. de' Medici, and J. Mravlje, *Annu. Rev. Condens. Matter Phys.* **4**, 137 (2013).
- [36] H. T. Dang, J. Mravlje, A. Georges, and A. J. Millis, *Phys. Rev. B* **91**, 195149 (2015).
- [37] P. G. de Gennes, *Phys. Rev.* **118**, 141 (1960).
- [38] S. Ishihara, J. Inoue, and S. Maekawa, *Phys. Rev. B* **55**, 8280 (1997).
- [39] H. Yi, J. Yu, and S.-I. Lee, *Phys. Rev. B* **61**, 428 (2000).
- [40] T. Ohsawa and J.-i. Inoue, *Phys. Rev. B* **65**, 134442 (2002).
- [41] H. Shinaoka, E. Gull, and P. Werner, *Comp. Phys. Comm.* **215**, 128 (2017).
- [42] D. Geffroy, A. Hariki, and J. Kunes, *ArXiv e-prints* (2018), [arXiv:1802.02387](https://arxiv.org/abs/1802.02387) [cond-mat.str-el].